Muon Spin Relaxation Study of the Spin Transition Compound $[Fe(Phen)_2(NCS)_2]$[⊥]

Y. Garcia,*,† V. Ksenofontov,‡ S. J. Campbell,§ J. S. Lord,|| Y. Boland,† and P. Gütlich‡

Unité de Chimie des Matériaux Inorganiques et Organiques, Département de Chimie, Faculté des Sciences, Université Catholique de Louvain, Place L. Pasteur 1, 1348 Louvain-la-Neuve, Belgium, Institut für Anorganische Chemie und Analytische Chemie, Universität Mainz, 55099 Mainz, Germany, School of Physical, Environmental and Mathematical Sciences, The University of New South Wales, Australian Defence Force Academy, Canberra, ACT 2600, Australia, and ISIS, Rutherford Appleton Laboratory, Chilton, Didcot, OX11 OQX, UK

Received: July 26, 2004; In Final Form: September 8, 2004

The thermal spin transition which occurs reversibly in $[Fe(phen)_2(NCS)_2]$ (polymorph I) around $T_{1/2} \sim 177$ K upon cooling and warming has been investigated by muon spin relaxation (μSR) measurements over the temperature range (∼10−280 K). The depolarization curves in zero and longitudinal fields (50−2000 Oe) are well described by two Lorentzian lines that represent fast and slow components in the decay curves and a nonrelaxing component. Evidence of the scope to track the spin transition occurring in $[Fe(phen)_2(NCS)_2]$ (polymorph I) is provided via the temperature dependence of the zero-field initial asymmetry parameter of the fast component. Muonium-substituted radicals delocalized on the phenanthroline ring (hyperfine coupling constant $A \sim 500$ MHz), as well as diamagnetic muonic species, have been identified on the basis of the applied field μSR experiments.

1. Introduction

Iron(II) spin transition (ST) materials continue to attract much interest with the focus centered on gaining a full understanding of their magnetic, optical, structural, and vibrational behavior.[1] The spin state of these compounds can be addressed on the molecular scale from high-spin (HS, $S = 2$) to low-spin (LS, $S = 0$) by various perturbations including temperature, electromagnetic radiation, and pressure.[2] These characteristics make these materials potentially significant in the emerging field of molecular electronics.[3] While the ST of iron(II) complexes has been widely investigated using numerous physical techniques,[4] muon spin relaxation (μSR) has only recently been applied in the study of ST materials.[5−9] In μSR spectroscopy, spin-polarized positive muons μ^+ are implanted into a sample thereby acting as probes of the local magnetization.[10−12] This provides information about magnetic fluctuations in a time window around 10^{-9} s to 10^{-5} s. This time scale is useful in the study of spin dynamics associated with spin transitions[13] and complements other techniques with different characteristic time windows.

$[Fe(phen)_2(NCS)_2]$ (phen = 1,10-phenanthroline) is known under the form of two polymorphs that both display a very abrupt ST around ∼177(1) K on cooling.[14,15] The magnetic properties of polymorph I differ from those of polymorph II; polymorph I presents a complete ST[16] whereas ∼17% of HS iron(II) ions are found in the low-temperature regime for polymorph II.[17,18] The crystal structure of $[Fe(phen)_2(NCS)_2]$ shows a mononuclear compound in which the iron(II) ion is surrounded by two phenanthroline rings and two thiocyanato anions arranged in the cis position, all coordinated through their nitrogen atoms (Figure 1). The mononuclear iron(II) units are linked in the crystal lattice by S···C and $\pi-\pi$ stacking interactions as found for polymorph II.[15] These intermolecular interactions between the iron(II) sites promote the steepness of the ST as well as the appearance of a hysteresis loop (∼1 K).[18,19] The ST of this material has been investigated thoroughly by a wide range of physical techniques. These include magnetic susceptibility, calorimetric measurements, XPS, X-ray diffrac-

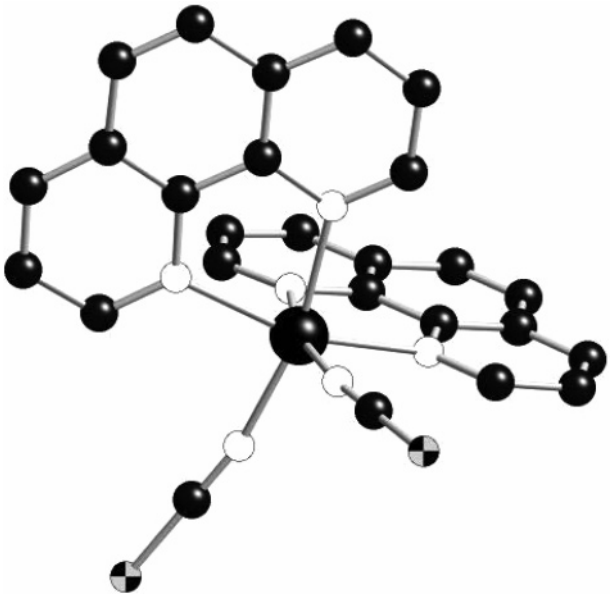

Figure 1. A view of the complex molecule of $[Fe(phen)_2(NCS)_2]$ at 293 K.[15] The large black sphere corresponds to an iron(II) ion and the smaller black, white, and the mixed black and white spheres correspond to carbon, nitrogen, and sulfur atoms, respectively (the hydrogen atoms have been omitted for clarity).

[⊥] This paper is dedicated to Professor Dr Philipp Gütlich by his coauthors on the occasion of his 70th birthday.

* To whom correspondence may be addressed. E-mail: garcia@chim.ucl.ac.be.

† Université Catholique de Louvain.

‡ Universität Mainz.

§ The University of New South Wales.

|| Rutherford Appleton Laboratory.

10.1021/jp046695y CCC: $27.50
Published on Web 10/22/2004

tion, X-ray absorption, ^{57}Fe Mössbauer, positron annihilation, UV, IR, Raman, and NMR spectroscopies with investigations also exploring the effects of metal dilution, pressure, magnetic fields, light, and soft X-ray irradiation on this thermal spin transition.[4] We have extended the scope of these earlier studies to the present investigation of the ST of $[Fe(phen)_2(NCS)_2]$ by muon spin relaxation.

Our earlier μSR study of $[Fe(ptz)_6](ClO_4)_2$ (ptz = 1-propyltetrazole) allowed us to track a thermal ST via the initial asymmetry parameter and the fast and slow decay constants. Analyses of the μSR and the related ^{57}Fe Mössbauer spectroscopy spectra led to new information on the lattice dynamic behavior occurring in $[Fe(ptz)_6](ClO_4)_2$.[7] By comparison, $[Fe(phen)_2(NCS)_2]$ can be considered as a model ST compound for investigation by μSR. $[Fe(phen)_2(NCS)_2]$ does not have any noncoordinated species—and thus fewer muon location sites—allowing scope for a more straightforward interpretation of its magnetic fluctuation behavior. The ST of $[Fe(phen)_2(NCS)_2]$ occurs over a narrower temperature range than $[Fe(ptz)_6](ClO_4)_2$. It is also free of complications because of HS-LS relaxation effects as demonstrated by ^{57}Fe Mössbauer spectroscopy measurements[20] or a structural phase transition accompanying the spin state change.[15] The completeness of the transition in $[Fe(phen)_2(NCS)_2]$ (polymorph I) allows three spin state ranges to be probed by μSR: a LS regime, an intermediate HS-LS, and a HS regime. The initial set of zero-field (ZF) μSR results on this compound and their analyses have recently been reported elsewhere.[21]

2. Experimental Section

$[Fe(phen)_2(NCS)_2]$ was synthesized as polymorph I using the procedure described elsewhere.[16] The μSR measurements were performed on the DEVA spectrometer at ISIS, Rutherford Appleton Laboratory, U.K. The powdered sample was inserted into an aluminum mount and covered with a Mylar film window. The holder was masked from the muon beam by a silver plate. The muons with energy ~3.2 MeV and implantation ranges about 100 mg cm^{-2} thermalize within the sample on time scales much shorter than the spin relaxation times.

The muons enter the sample with their polarization antiparallel to the beam direction, chosen as the *z* direction, and decay with a mean lifetime of 2.2 μs, emitting positrons preferentially along the muon spin direction that are detected by scintillation detectors which surround the sample. The asymmetry is described by the following function with a_o being the initial asymmetry, $G_z(t)$ the depolarization function, N_F and N_B, the number of the decay positrons detected by the forward and backward counters, respectively, and α an experimental calibration constant that is dependent on sample position and detector efficiencies:

$$a(t) = a_0\, G_z(t) = \frac{N_F(t) - \alpha N_B(t)}{N_F(t) + \alpha N_B(t)} \qquad (1)$$

The μSR data were recorded in longitudinal geometry over the temperature range ~10−280 K using an OXFORD instruments He flow cryostat and analyzed using the WIMDA software.[22]

3. Results

The $[Fe(phen)_2(NCS)_2]$ sample was cooled slowly to 10 K to prevent any thermal trapping of the HS state. Zero-field as well as longitudinal field (LF) (50−2000 Oe) μSR spectra were subsequently recorded at selected temperatures on a warming mode up to 280 K. Figure 2 shows the ZF and LF (2000 Oe) μSR spectra obtained at 10 and 280 K, below and above $T_{1/2}$ ~ 177 K, respectively. The relaxation spectra are typical of the behavior of $[Fe(phen)_2(NCS)_2]$ and generally reveal a region of fast relaxation occurring over the first few μs, followed by a slower relaxation behavior. As evident from Figure 2, relatively little change is observed in the initial asymmetry at 280 K when the field is applied compared with the results obtained at 10 K as discussed below. The ZF and LF-μSR spectra were both fitted best with two Lorentzian components over the temperature range of investigation (~10−280 K) using the following asymmetry function:

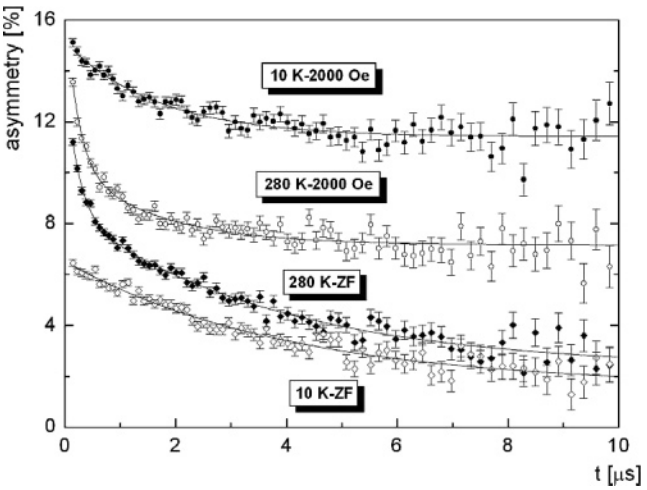

Figure 2. Representative ZF and LF-2000 Oe μSR curves for $[Fe(phen)_2(NCS)_2]$ at 280 K and 10 K. The lines represent fits to the data as explained in the text.

$$a(t) = a_s e^{-\lambda_s t} + a_f e^{-\lambda_f t} + a_{nr} \qquad (2)$$

a_s and a_f represent the amplitudes of the asymmetry of slow and fast components, respectively, and a_{nr} represents the amplitude of a nonrelaxing component taking into account the background and quenched paramagnetic muons in the presence of an applied magnetic field. λ_s and λ_f are the decay constants of the slow and fast components, respectively.

λ_s was constant, $\lambda_s \sim 0.25(3)\ \mu s^{-1}$, over the temperature range ~10−280 K. λ_f was essentially temperature independent in the HS state above ~200 K although irregular values for λ_f were obtained from ~200 K to 10 K. The best fits to the ZF-μSR spectra were obtained with λ_f fixed to the value obtained at the highest recorded temperature (280 K, $\lambda_f \sim 4.53\ \mu s^{-1}$). The use of a Gaussian line did not result in improved fits to the ZF-μSR spectra (even over the LS temperature range ~10−100 K), contrary to results reported previously for $[Fe(phen)_2(NCS)_2]$.[5]

Figure 3 shows the variation of the initial asymmetry parameter, a_o, over the temperature range ~10−280 K. a_0 remains approximately constant at ~7% for $T \leq 125$ K, increasing to the approximately constant value of ~14% for $T \geq 225$ K. The temperature dependences of the slow and fast components of the initial asymmetry, a_0^s and a_0^f, respectively, are also shown in Figure 3. The slow component of the initial asymmetry parameter increases gradually from ~5% at 10 K to ~6% at 280 K whereas the fast component of the initial asymmetry parameter remains effectively constant at ~0−1% over the range ~10−125 K before increasing to a value of ~5.5% above 225 K. As demonstrated in Figure 4, the temperature variation of a_0^f correlates well with the warming magnetic susceptibility measurements (the $\chi_M T$ values[15] were normalized to the a_0^f value at 280 K) although slight deviations

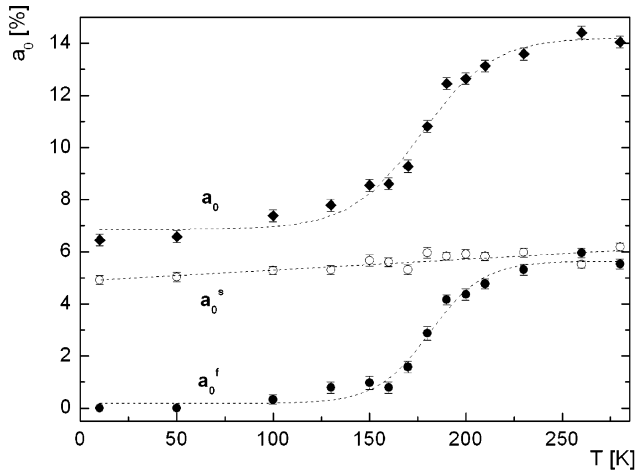

Figure 3. The dependence of the initial asymmetry parameter, a_o, (◆) on temperature for $[Fe(phen)_2(NCS)_2]$. The temperature dependences of the slow, a_0^s (○), and fast, a_0^f (●), components of the asymmetry parameter are also shown. The dashed curves act as guides to the eye.

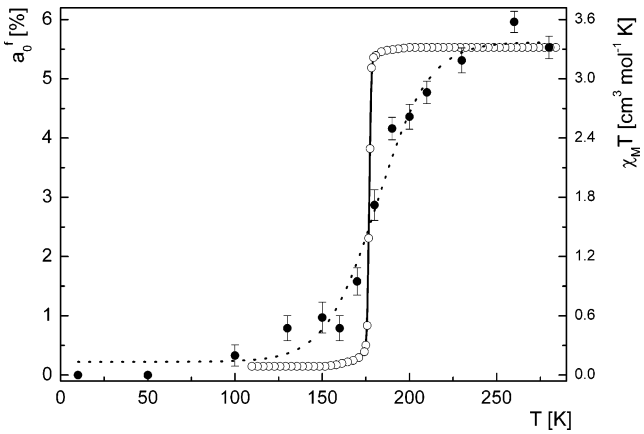

Figure 4. A comparison between the temperature dependences of $\chi_M T$ (○) (right scale, adapted from ref 15) and the fast asymmetry parameter a_0^f in zero field (●) (left scale) for $[Fe(phen)_2(NCS)_2]$ on warming from 10 K (the dashed line shows the trend of the a_0^f data). The $\chi_M T$ values have been normalized to the value of a_0^f at 280 K.

in the overlap between the $\chi_M T$ and a_0^f curves are observed in the regions just above and below $T_{1/2}$ from ∼225−177 K and ∼177−125 K, respectively. As is evident in Figure 4, the transition temperature evaluated from μSR $T_{1/2} = 178(2)$ K agrees well with the value $T_{1/2} = 177(1)$ K determined from the magnetic susceptibility measurements.

Figure 5 shows the ZF and 20 Oe transverse field (TF) relaxation curves obtained at 280 K (above $T_{1/2}$) and 10 K (below $T_{1/2}$). The TF μSR spectra were fitted best using the asymmetry function:

$$a(t) = (a_s\, e^{-\lambda_s t} + a_f\, e^{-\lambda_f t} + a_{bg}) \cos(\omega t + \varphi) \qquad (3)$$

where ω represents the precession frequency and φ the phase. The ZF and TF curves at these high and low temperatures have approximately the same initial asymmetry (∼14% at 280 K, ∼7% at 10 K) with the ZF and TF curves also found to exhibit similar relaxation rates ($\lambda_s \sim 0.26\ \mu s^{-1}$ at 280 K; $\lambda_s \sim 0.31\ \mu s^{-1}$ at 10 K). The TF relaxation curves at both temperatures have a precession frequency ω of 135.5 MHz T^{-1}, characteristic of diamagnetic muon.[10]

The isothermal relaxation spectra recorded at LF (50−2000 Oe) at selected temperatures over the range 10−280 K were fitted to eq 2 to derive the repolarization data $a_o(B)$, shown in

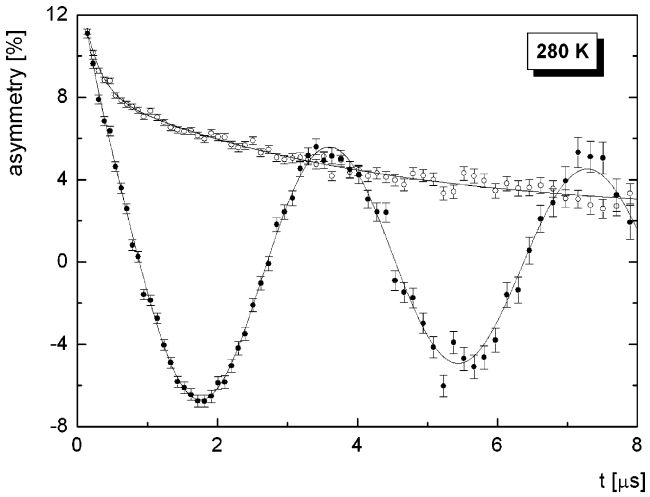

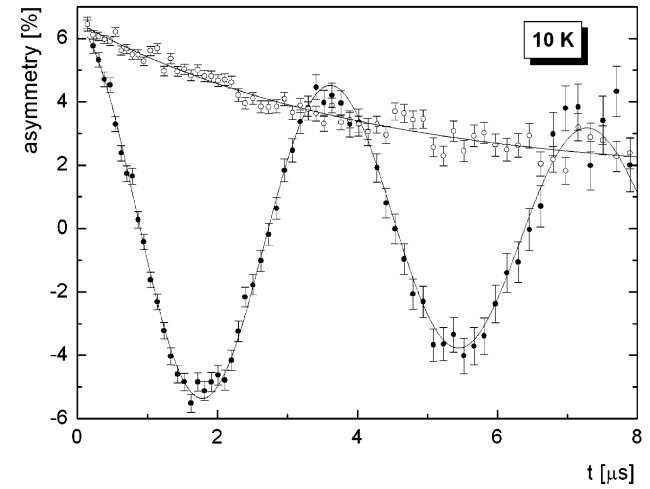

Figure 5. Comparison between the ZF (○) and TF-20 Oe relaxation curves (●) at 280 K (upper) and 10 K (lower) for $[Fe(phen)_2(NCS)_2]$. The lines represent fits to the data as explained in the text.

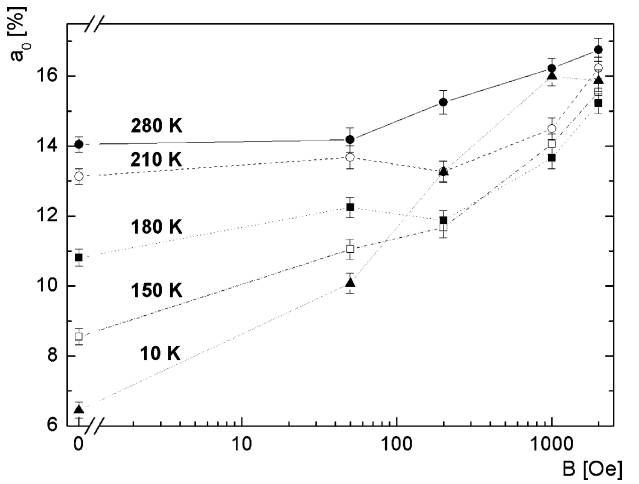

Figure 6. Dependence of the initial asymmetry parameter, a_0, of $[Fe(phen)_2(NCS)_2]$ on magnetic field, B, up to 2000 Oe at the temperatures indicated [▲, $T = 10$ K; □, $T = 150$ K; ■, $T = 180$ K; ○, $T = 210$ K; ●, $T = 280$ K]. The lines act as guides to the eye.

Figure 6. The shape of the repolarization curves obtained on connecting the data points for low fields ($B \leq 50$ Oe) shows a tendency for a more abrupt change at low fields as the temperature decreases, whereas within error, a tendency toward saturation in a_0 is observed at higher fields, $B \geq 1000$ Oe. This behavior of the initial asymmetry $a_o(B)$ as a function of magnetic

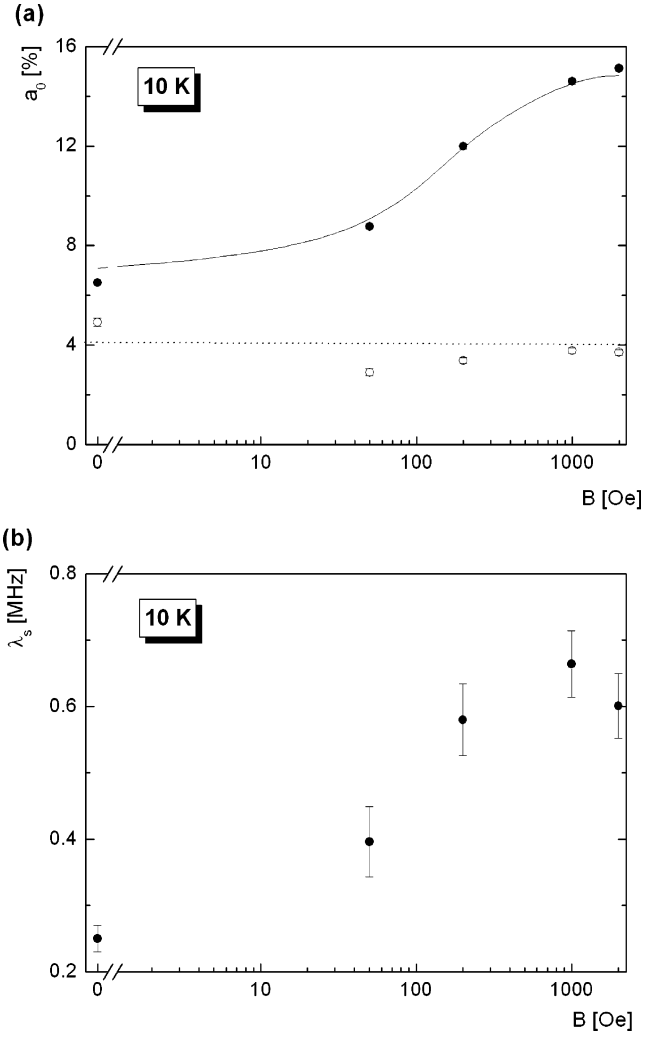

Figure 7. (a) Dependence of a_0 (●) and a_o^s (○) on magnetic field for $[Fe(phen)_2(NCS)_2]$ at 10 K. The line acts as a guide to the eye. The dotted line represents the average value of a_0^s and corresponds to a diamagnetic contribution $a_{dia} \sim 4\%$ as discussed in the text. (b) Dependence of the relaxation rate, λ_s, on magnetic field for $[Fe(phen)_2(NCS)_2]$ at 10 K.

field (increase in $a_o(B)$ below 210 K, reaching saturation above 1000 Oe) provides evidence for the formation of a paramagnetic state such as muonium $Mu^{\bullet} = \mu^+e^-$, an analogue of atomic hydrogen. By comparison, in low-field values, $B \leq 50$ Oe, and above 210 K, the presence of a fraction of paramagnetic muonium is not clearly revealed because of its very high relaxation rate. At very high fields, $B \geq 1000$ Oe, any paramagnetic muonium present would be repolarized when the Larmor frequency of the electron exceeds the hyperfine coupling of an electron and a muon. As evident in Figure 6 for the 10 K curve, a_0 increases significantly above ~50 Oe, resulting in the data crossing the repolarization curves recorded at higher temperatures. This behavior could be the signature of another radical which is coupled weakly or it could be considered as an artifact as a consequence of the fluctuation frequency of the iron atoms.

These repolarization data were fitted to the isotropic repolarization function given by eqs 4 and 5:

$$a_0(B) = a_{dia} + a_{para}\left(1 + \frac{x^2}{x^2+1}\right) \quad (4)$$

$$\text{where } x = (\gamma_e - \gamma_\mu)\frac{B}{A} \quad (5)$$

a_{dia} and a_{para} represent the diamagnetic and paramagnetic contributions, respectively, in an applied field.[10] $\gamma_e = 28$ GHz T^{-1} and γ_μ is the muon gyromagnetic ratio (135.5 MHz T^{-1}). A was not fixed during the fit and was assumed to be independent of temperature. Analysis of all the repolarization data over the temperature range ~10−280 K resulted in a value for the hyperfine coupling constant of $A \sim 500$ MHz.

Equation 2 was also used to derive the decay constants of the slow and fast components, λ_s and λ_f. These fits demonstrate that λ_s and λ_f are essentially field independent. Given that $a_0^f \sim 0\%$ at 10 K (see Figure 3), a further fit to the LF-μSR spectrum was carried out using a simplified version of eq 2 which included only the slow Lorentzian component, $a_s e^{-\lambda_s t}$, and the nonrelaxing component, a_{nr}. As shown by Figure 7a, a_0^s is essentially field independent whereas a_{nr} exhibits a gradual increase with magnetic field. The dotted line in Figure 7a represents the average value of a_0^s, corresponding to a diamagnetic contribution $a_{dia} \sim 4\%$. At 10 K, the relaxation rate increased gradually from $\lambda_s \sim 0.25\ \mu s^{-1}$ at $B = 1$ Oe to $\lambda_s \sim 0.6\ \mu s^{-1}$ for $B \geq 2000$ Oe (Figure 7b).

4. Discussion

The overall temperature dependence of the initial asymmetry parameter of $[Fe(phen)_2(NCS)_2]$ can be separated into a slow and a fast component (Figure 3). We attribute the variation of a_o^s to diamagnetic muons that are present over the entire temperature range as demonstrated by comparison of the ZF 20 Oe and TF relaxation curves at 280 and 10 K (Figure 5). A large fraction of muons must however remain paramagnetic over the whole temperature range as shown by the initial asymmetry parameter varying from ~7% to ~14% between 10 and 280 K, respectively, compared with the maximum initial asymmetry of our μSR spectrometer of ~21%. Indeed, the occurrence of the paramagnetic species is confirmed by the field dependence of the initial asymmetry parameter (Figure 6). These paramagnetic species are present in the form of muonium radicals as indicated by the unsaturated character of phen in $[Fe(phen)_2(NCS)_2]$ and the hyperfine constant of ~500 MHz—the same value as for polystyrene.[23] Such radical species were also identified for benzene and for the coordination compound $[Fe(ptz)_6](ClO_4)_2$, with similar hyperfine constants of $A \sim 514.6$ MHz[24] and 540 MHz,[7] respectively, being obtained. By comparison, this value for A in $[Fe(phen)_2(NCS)_2]$ is much lower than that found for a free muonium atom ($A \sim 4463$ MHz).[25]

Below 100 K, where all Fe(II) are in a diamagnetic LS state,[17] the ZF a_0 values correspond to that of diamagnetic muons perturbed by the local nuclear moments of atoms of the crystal matrix. This allows paramagnetic muonium radicals to interact with the static internal magnetic fields created by the nuclear dipole moments of the lattice atoms. As the temperature increases through the ST region above 125 K, the proportion of Fe(II) ions switching from the diamagnetic LS state to the paramagnetic HS state increases, thereby allowing an interaction between the electronic spins of muonium and the spins of the Fe(II) ion in the HS state. The repolarization curves recorded above $T_{1/2} = 178(2)$ K show that full asymmetry is attained but with a weak magnetic field dependence (Figure 6). This behavior indicates that diamagnetic-like muonium states as well as diamagnetic muons are present in the HS state of $[Fe(phen)_2(NCS)_2]$. Since a_0^s remains relatively constant, the increase in the fraction of the diamagnetic-like muonium states upon warming from ~125 K as shown by a_0^f (Figure 4), can be understood if the dynamic character of paramagnetic spins in the HS phase which are coupled strongly to the muonium

electron is considered. Through the ST region (~125−225 K), the iron spin and the muonium electron spin are coupled and have a sufficiently high relaxation rate to decouple the electron from the muon. This results in an unusual diamagnetic behavior observed for the muons in the paramagnetic surroundings of the HS state of $[Fe(phen)_2(NCS)_2]$. This presumes a strong spin−spin interaction between the electron of the radical and the unpaired electrons of the complex in the HS state. This spin−spin interaction is stronger than the strength of the muon hyperfine interaction and causes the electron spin to fluctuate sufficiently rapidly to decouple it from the muon. Indeed, as the temperature increases, the relaxation frequency of the spins of the iron complexes increases. Since we have both diamagnetic and paramagnetic fractions at 280 K, as a result of its radical nature, the faster-relaxing component has the extra relaxation $\lambda = \lambda_f - \lambda_s \sim 4.3\ \mu s^{-1}$. Hence, assuming a similar nuclear relaxation rate constant for the fast and slow components, this results in an electron fluctuation rate of $\nu = A^2/\lambda \sim 58$ GHz at 280 K, with $A \sim 500$ MHz as determined above.

Here, we consider the location of the different muon species in $[Fe(phen)_2(NCS)_2]$. As indicated above and discussed below, we have found evidence for the presence of muonium radicals in $[Fe(phen)_2(NCS)_2]$. Such species are expected to form when muons are added to organic molecules with unsaturated bonds,[26] such as phen in the present case. This is demonstrated, for example, by the important muonium reaction rate constant of $1.3 \times 10^9\ M^{-1}\ s^{-1}$ for naphthalene.[27] The addition of muons results in the formation of muonium species with the unpaired electron spin localized in an orbital of p or π symmetry.[28] As depicted below (see also Figure 1), several locations can be suggested for the muonium substituted radicals in *cis*-$[Fe(phen)_2(NCS)_2]$, that is, bonded to a C, N, or S atom.

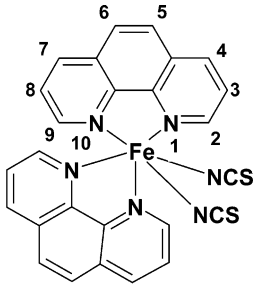

The bonding of muonium to a N atom belonging to the phenanthroline ring or to the anion would require the muon to be close to the Fe(II) ion, which is unlikely for steric reasons. Also, a variation of the crystal field strength would be expected which would modify the thermal ST curve. However, as demonstrated by Figure 4, a close correspondence has been observed between the magnetic data and the ZF initial fast asymmetry parameter. The bonding of muonium to the C or S atom of the anion can also be considered, with the addition of Mu· to the C═S bond still being debated.[28,29] This position seems to be unlikely, however, since recent LF-μSR experiments carried out on iron(II) mononuclear complexes of the $[FeL_2(NCS)_2]$ type that contain thiocyanato anions in the cis position around the iron(II) ion[30] have demonstrated the absence of muonium species.[8] The bonding of muonium to a C atom of the phen ligand creates muonated species with a radical delocalized on the phenanthroline ring. Positions 2−5 in the above diagram can thus be considered as well as positions with multiple occupation (e.g., 4,7; 3,4,7,8; ...). However, positions 2 and 9 are less favored for steric reasons. Such sets of localizations would, however, alter markedly the electronic structure and thus the magnetic properties of the Fe(II) compound as was found for the series of $[Fe(Y\text{-}phen)_2(NCS)_2]$ complexes with Y = Me, Cl, NO_2.[31] Also, these positions are considered to be very unlikely for statistical reasons.[12] Transverse field muonium spectra or preferably resonance field μSR measurements would be useful to gain insight to the localization of muons in $[Fe(phen)_2(NCS)_2]$ and to allow the hyperfine coupling parameters of the radical states to be obtained more accurately.

Paramagnetic species can also be present as "free" interstitial muonium or as muonium radicals that are not decoupled by the HS Fe(II) spin. In this instance, some muon sites on the phen ring may have a very weak coupling to the Fe(II) spins, for example, with the muon occupying positions 5 or 6. The present *A* value can only be considered as a first approximation since the isotropic repolarization function (eq 4) does not match the repolarization data below 180 K, a deviation that is more evident at 10 K. Indeed, this discrepancy suggests that the hyperfine interaction is presumably not isotropic in $[Fe(phen)_2(NCS)_2]$; this suggests these data should be considered in the frame of an appropriate anisotropic model.[32] In comparison with $[Fe(ptz)_6](ClO_4)_2$, diamagnetic muons species are expected to be located closer to the Fe spins in $[Fe(phen)_2(NCS)_2]$ which do not contain any uncoordinated species. These positive muons should, however, be repelled by Fe(II) cations and probably attracted by more negative sites such as the sulfur or nitrogen atom of the anions. This would explain the higher values of the relaxation constant in $[Fe(phen)_2(NCS)_2]$ ($\lambda_s \sim 0.25\ \mu s^{-1}$ and $\lambda_f \sim 4.53\ \mu s^{-1}$) compared to the values found for $[Fe(ptz)_6](ClO_4)_2$ ($\lambda_s^{max} \sim 0.15\ \mu s^{-1}$ and $\lambda_f^{max} \sim 2\ \mu s^{-1}$).[7] Also, the presence of "free" interstitial diamagnetic muons species cannot be totally excluded.

As demonstrated by Figure 4, there is a clear connection between the gradients of the ST curve derived from magnetic susceptibility measurements and a_0^f. The variation of a_0^f thus indicates the fraction of the muoniums that interacts with unpaired spins and therefore the fraction of the HS molecules present at any temperature. The observed deviations between the magnetic susceptibility measurement and the muon response suggest that the muonium radical interacts with more than one HS molecule in the crystal lattice of $[Fe(phen)_2(NCS)_2]$. These deviations do not indicate that the cooperative effects associated with the spin state transition are necessarily lost, as the Fe spin interacting with the muon is still also interacting with neighboring Fe(II) spins, lattice strain, and so forth. Also, for the present material, the cooperative effects have been mostly attributed to the presence of $\pi-\pi$ stacking interactions that link the mononuclear iron(II) units of $[Fe(phen)_2(NCS)_2]$ in the crystal lattice.[19] These supramolecular interactions are unlikely to be affected by the presence of the muon. This difference in the response of the two techniques through the ST region could also be explained by the different techniques used to detect the spin transition. Given the slow time scale of the $\chi_M T$ measurements compared with that of μSR, average concentrations of the HS fractions are sensed in the magnetization measurements leading to the appearance of a relatively sharp spin transition. On the other hand, the shorter μSR time scale enables fluctuations because of the fractions of HS occurring around $T_{1/2}$ to be detected; this leads to the broader temperature range over which the ST is sensed by μSR as depicted by the a_0^f values in Figure 4. Indeed, if the individual spins are flipping between HS and LS more rapidly than the muon lifetime ($\tau_\mu = 2{,}2\ \mu s$), the average μSR data may be weighted more toward the

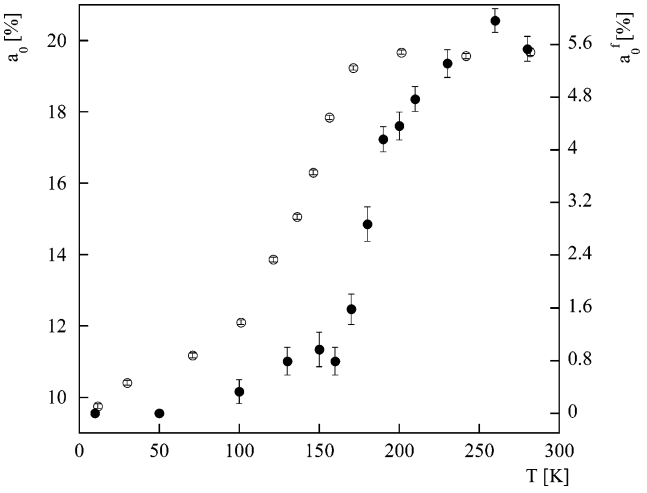

Figure 8. A comparison between the temperature dependences of the initial asymmetry parameter in zero field, a_o, for $[Fe(ptz)_6](ClO_4)_2$ (○) (left scale) and the fast asymmetry parameter in zero field, a_0^f, for $[Fe(phen)_2(NCS)_2]$ (●) (right scale) on warming from 10 K. The a_0 values have been normalized to the value of a_0^f at 280 K.

occasional preference of either the HS or the LS state, rather than proportional to the HS fraction.

As the transition temperature, $T_{1/2} = 178(2)$ K, obtained from the μSR experiments matches that from other techniques, $T_{1/2} = 177(1)$ K, and there is no evidence for other transitions in the μSR data, it is considered to be unlikely that the muon would cause a significant local perturbation to the SCO compound. Macroscopic effects are also unlikely for statistical reasons as the concentration of thermalized species is negligible. Another factor that could account for the deviations around $T_{1/2}$ between the ST curves derived from the $\chi_M T$ and a_0^f measurements would be a possible preference for the "free" diamagnetic muons species to be located in defect sites, such as surfaces sites. Such a situation is unlikely at low temperatures, however, where the muon does not have enough thermal energy to diffuse although diffusion could play a role at higher temperatures. Diffusion cannot be considered as the origin of the difference in the present case, however, as a_0^f reflects the fraction of diamagnetic-like muonium states that are linked to the complex molecule and that thus do not diffuse.

Comparison of the ST curves as derived by μSR for $[Fe(phen)_2(NCS)_2]$ and $[Fe(ptz)_6](ClO_4)_2$ [7] (Figure 8) reveals that the spin transition of $[Fe(phen)_2(NCS)_2]$ occurs over a relatively narrow temperature range compared with $[Fe(ptz)_6](ClO_4)_2$[7] (this behavior is also mirrored by the trends of the magnetic data). This relative behavior demonstrates that the thermally induced spin state transition has been tracked more accurately by μSR in $[Fe(phen)_2(NCS)_2]$ than in $[Fe(ptz)_6](ClO_4)_2$ since the fraction of diamagnetic muons as represented by a_o^s (and whose respective amount increases slightly from ~10 K to 280 K) could be extracted from the total initial asymmetry.

5. Conclusions

The reversible HS to LS transition which occurs in $[Fe(phen)_2(NCS)_2]$ around $T_{1/2} \sim 177$ K has been investigated by ZF-μSR measurements over the temperature range ~10−280 K. The initial asymmetry parameter can be described in terms of contributions from slow and fast components (Figure 3) with the initial asymmetry parameter of the fast component found to track the spin transition around the transition temperature $T_{1/2} = 178(2)$ K determined from the μSR measurements. The broader temperature range over which the ST takes place as observed by μSR compared with magnetic susceptibility measurements (Figure 4) reflects the different measurement time scales and the interaction of a fraction of next-nearest HS Fe(II) complexes with the muons.

Several muonic species have been discussed in $[Fe(phen)_2(NCS)_2]$ and their interactions and locations considered. A fraction of diamagnetic muons exists over the temperature range ~10−280 K, as evidenced by the initial asymmetry parameter of the slow component, with the existence of diamagnetic-like and paramagnetic muonium-substituted radicals delocalized on the phenanthroline ring revealed by the LF-μSR repolarization data.

The μSR measurements with their characteristic time scale associated with the muon lifetime have enabled fluctuations between the HS and LS states occurring around $T_{1/2}$ in $[Fe(phen)_2(NCS)_2]$ to be sensed, whereas these fluctuations are not evident in the magnetic susceptibility and ^{57}Fe Mössbauer spectroscopy[20] measurements. Muon spin relaxation thus offers a powerful technique for probing the dynamic phenomena occurring in ST compounds. Investigations of a series of materials which exhibit a range of different spin transition behaviors by μSR are continuing.

Acknowledgment. We acknowledge support from the European Union under Framework 5 for access to the DEVA instrument at the ISIS Facility, Rutherford Appleton Laboratory, U.K. S.J.C. acknowledges support from the Access to Major Research Facilities Program, Australian Nuclear Science and Technology Organization. We thank the Fonds pour la Formation à la Recherche dans l'Industrie et dans l'Agriculture for a doctoral scholarship allocated to Y.B. We also thank the Deutsche Forschungssgemeinschaft (Priority Program No.1137 "Molecular Magnetism"), the Fonds der Chemischen Industrie, the Materialwissenschaftliches Forschungszentrum of the University of Mainz, and the Fonds Special de Recherche of the University of Louvain for financial help.

References and Notes

(1) Gütlich, P.; Hauser, A.; Spiering, H. *Angew. Chem., Int. Ed. Engl.* **1994**, *33*, 2024.

(2) Gütlich, P.; Garcia, Y.; Goodwin, H. A. *Chem. Soc. Rev.* **2000**, *29*, 419.

(3) Kahn, O.; Jay-Martinez, C. *Science* **1998**, *279*, 44.

(4) Gütlich P.; Garcia, Y.; Spiering, H. In *Magnetism: From Molecules to Materials*; Miller, J. S., Drillon, M., Eds.; Wiley-VCH: Verlag GmbH; Weiheim, 2003; Vol. IV, p 271.

(5) (a) Shioyasu, N.; Kagetsu, K.; Mishima, K.; Kubo, M. K.; Tominaga, T.; Nishiyama, K.; Nagamine, K. *Hyperfine Interact.* **1994**, *84*, 477. (b) Kubo, M. *Anal. Sci.* **2001**, *17* (Suppl. i653).

(6) Campbell, S. J.; Ksenofontov, V.; Garcia, Y.; Lord, J. S.; Reiman, S.; Gütlich, P. *Hyperfine Interact. C* **2002**, *5*, 363.

(7) Campbell, S. J.; Ksenofontov, V.; Garcia, Y.; Lord, J. S.; Boland, Y.; Gütlich, P. *J. Phys. Chem. B* **2003**, *107*, 14289.

(8) (a) Blundell S. J.; Pratt F. L.; Lancaster, T.; Marshall I. M.; Steer C. A.; Heath S. L.; Létard, J.-F.; Sugano, T.; Mihailovic, D.; Omerzu, A. *Polyhedron* **2003**, *22*, 1973. (b) Blundell, S. J.; Pratt, F. L.; Steer, C. A.; Marshall, I. M.; Létard, J.-F. *J. Phys. Chem. Solids* **2004**, *65*, 25.

(9) Roubeau, O.; Gubbens, P. C. M.; Visser D., Blaauw, M.; Dalmas de Réotier, P.; Yaouanc, A.; Haasnoot, J. G.; Reedijk, J.; Sakarya, S.; Jayasooriya, U. A.; Cottrell, S. P.; King, P. J. C. *Chem. Phys. Lett.* **2004**, *395*, 177.

(10) Cox, S. F. J. *J. Phys. C: Solid State Phys.* **1987**, *20*, 3187.

(11) Muon Science: Muons in Physics, Chemistry and Solids. In *Proceedings of the 51st Scottish Universities Summer School in Physics;* Lee S. L., Kilcoyne, S. H., Cywinski, R., Eds.; A Nato Advanced Study Institute, Institute of Physics, Vol. 51, 1998.

(12) Blundell, S. J. *Contemp. Phys.* **1999**, *40*, 175.

(13) König, E. *Struct. Bonding* **1991**, *76*, 51.

(14) Baker, W. A.; Bobonich, H. M. *Inorg. Chem.* **1964**, *3*, 1184.

(15) Gallois, B.; Real, J. A.; Hauw, C.; Zarembowitch, J. *Inorg. Chem.* **1990**, *29*, 1152.

(16) (a) König, E.; Madeja, K. *Inorg. Chem.* **1967**, *6*, 48. (b) Deszi, I.; Molnar, B.; Tarnoczi, T.; Tompa, K. *J. Inorg. Nucl. Chem.* **1967**, *29*, 2486.

(17) Ganguli, P.; Gütlich, P.; Müller, E. W.; Irler, W. *J. Chem. Soc., Dalton Trans*. **1981**, 441.

(18) Müller, E. W.; Spiering, H.; Gütlich, P. *Chem. Phys. Lett*. **1982**, *93*, 567.

(19) Real, J. A.; Gaspar, A. B.; Niel, V.; Carmen Muñoz, M. *Coord. Chem. Rev*. **2003**, *236*, 121.

(20) Ganguli, P.; Gütlich, P.; Müller, E. W. *J. Chem. Soc., Dalton Trans*. **1981**, 441.

(21) Garcia, Y.; Ksenofontov, V.; Campbell, S. J.; Lord, J. S.; Boland, Y.; Gütlich, P. *Phys. Status Solidi* (Proc SCM2004, in press).

(22) Pratt, F. L. *Physica B* **2000**, *289*−*290*, 710.

(23) Pratt, F. L.; Blundell, S. J.; Marshall, I. M.; Lancaster, T.; Husmann, A.; Steer, C.; Hayes, W.; Fischmeister, C.; Martin, R. E.; Holmes, A. B. *Physica B* **2003**, *326*, 34.

(24) Roduner, E.; Fischer, H. *Chem. Phys. Lett*. **1979**, *65*, 582.

(25) Casperson, D. E.; Crane, T. W.; Denison, A. B.; Egan, P. O.; Hughes, V. W.; Mariam, F. G.; Orth, H.; Reist, H. W.; Souder, P. A.; Stambaugh, R. D.; Thompson, P. A.; Zu, G. *Phys. Rev. Lett.* **1977**, *38*, 956.

(26) Walker, D. W. *Muon and muonium chemistry*; Cambridge University Press: New York, 1984.

(27) Jean, Y. C.; Ng., B. W.; Stadlbauer, J. M.; Walker, D. C. *J. Chem. Phys*. **1981**, *75*, 561.

(28) Macrae, R. M.; Carmichael, I. *J. Phys. Chem*. *A* **2001**, *105*, 3641.

(29) Macrae, R. M.; Carmichael, I. *Physica B* **2003**, *326*, 81.

(30) Guionneau, P.; Létard, J. F.; Yufit, D. S.; Chasseau, D.; Bravic G.; Goeta, A. E.; Howard, J. A. K.; Kahn, O. *J. Mater. Chem*. **1999**, *9*, 985.

(31) Gütlich, P. *Struct. Bonding (Berlin)* **1981**, *44*, 83.

(32) Risch, R.; Kehr, K. W. *Phys. Rev. B* **1992**, *46*, 5246.